THE ANNALS OF "DUNĂREA DE JOS" UNIVERSITY OF GALAȚI
FASCICLE V, TECHNOLOGIES IN MACHINE BUILDING,
ISSN 1221- 4566, 2011

COMPARATIVE ANALITICAL MODELS FOR SHARPENING OF MULTI FLUTE DRILLS WITH CURVED CUTTING EDGES

Eng. Baroiu Nicusor[1], PhD. Eng. Teodor Virgil[1],
Eng. Dumitraşcu Nicu[1], PhD. Eng. Oancea Nicolae[1]

[1] "Dunărea de Jos" University of Galaţi, Romania
Nicusor.Baroiu@ugal.ro

ABSTRACT

In this paper, are presented analytical models of the flank faces of multi flute drills. Are analysed quantitative differences regarding the sharpening quality by variation law of flank angle along the major cutting edge. Numerical examples are presented.

KEYWORDS: hyperboloidal sharpening, numerical modelling, multi flute drills, curved cutting edges, models for sharpening

1. Introduction

For helical drills with curved cutting edges, created in order to uniformize the unitary energetical load along the major cutting edge, [2, 3], (see Figure 1) were imaginated some specifically sharpening methods: thoroidal sharpening [2], as well as, for multi flute drills, variants of conical sharpening [3]; cylindrical [4] and hyperboloidal sharpening [1].

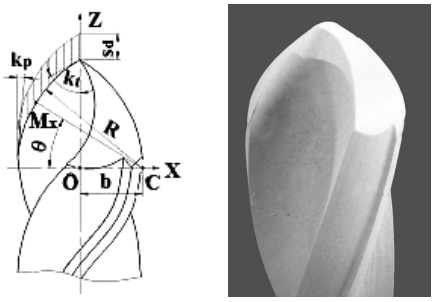

Fig. 1. *Multi flute drill with curved cutting edge*

There are some differences between these sharpening methods, regarding the generation kinematics and the results of flank face of the drill's major cutting edge.

If it is ensured the same geometry of the major cutting edge — the same variation law of the tool cutting edge angle, along the major cutting edge, the specifically sharpening method (cylindrical, conical or hyperboloidal) may lead to different values of the flank angle along the cutting edge and, in the same time, of the relieved flank surface, as it is presented by analytical models of the sharpening methods for straight lined cutting edge drills.

This paper proposes an analytical modeling of the geometrical surface which represents the flank faces of the curved cutting edge drills, for three of the presented methods (hyperboloidal, cylindrical and conical), the determination of the flank angle value, along the major cutting edge and, based on a specific software, the numerical determination of the variation law for the flank angle value along the major cutting edge, in order to make a comparison between the proposed sharpening methods.

The comparison between the sharpening process is made in conditions of the identical geometry of the major cutting edge, for all of the three proposed sharpening methods.

The analytical modeling, with numerical finalization of the flank angle value variation law, along the major cutting edge, may constitute a way to characterize other sharpening methods, as well as, for the evaluation of the reliev of the flank surface, as major aspect in order to establish the sharpening method quality.

2. Sharpening methods kinematics

It is analyzed the kinematics of sharpening methods for helical drills with curved cutting edges such as: hyperboloidal sharpening; conical sharpening and cylindrical sharpening.

In Figure 2, is presented the generation kinematics for hyperboloidal sharpening and the position of the sharpened drill regarding this surface.

The sharpening method using a hyperboloidal surface consists in the successive forming of the hyperboloidal surfaces of the flank faces *a, b, c,* using an external cylindrical surface *d* of a grinding wheel, which execute a rotation *A* around its own axis.

The flank surface sharpening of a cutting edge is made by composing a swing motion *B* of the drill, whose axis is perpendicular to the swing axis and is excentrical with value *e* regarding this axis, with an axial feed and intermittent motion *C*, which ensure the relieving of the flank surface, at a single positioning of the sharpened drill. In order to sharpen the flank surfaces *b* and *c* of the another teeth of the drill it is necessary to rotate the drill with 120°, and respectively 240°, resulting a circle arc cutting edge *f*.

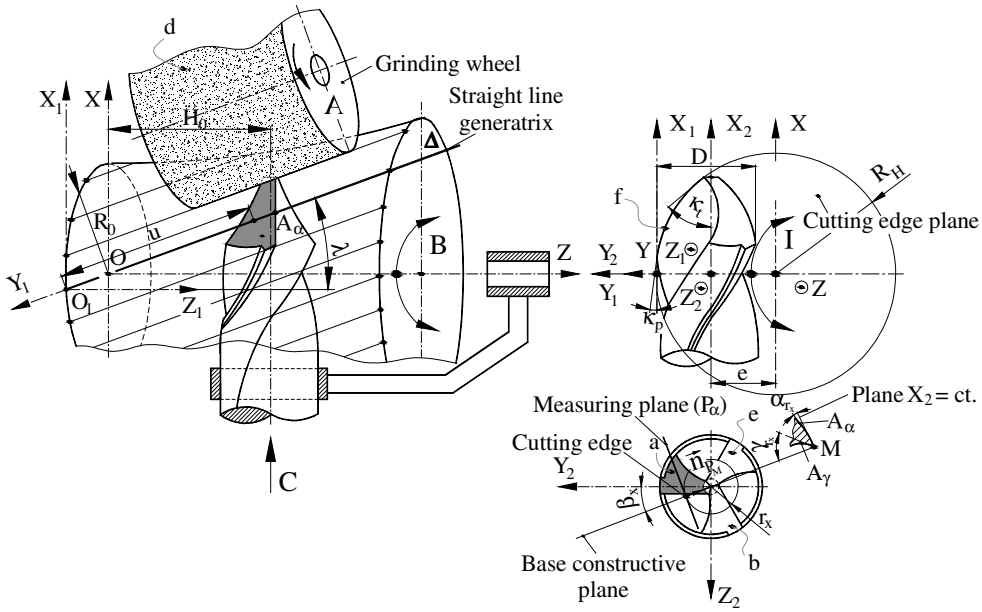

Fig. 2. *The generation kinematics for hyperboloidal sharpening*

The sharpening method using a conical surface consists in the successive forming of the conical surfaces of the flank faces *a, b, c,* using a frontal surface *d* of a grinding wheel, which execute a rotation *A* around its own axis, Figure 3.

The flank surface sharpening of a cutting edge is made by composing a swing motion *B* of the drill, whose axis is perpendicular on the swing axis and motion *C*, which ensure the relieving of the flank surface, at a single positioning of the sharpened drill.

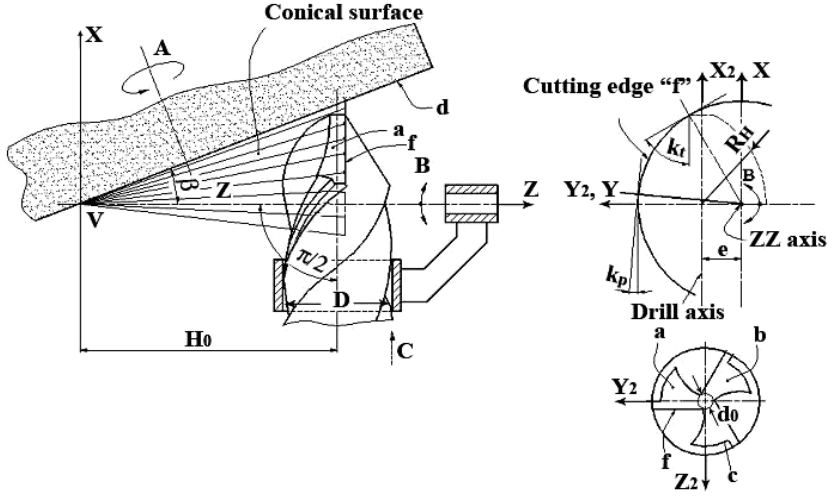

Fig. 3. *The generation kinematics for conical sharpening*

The sharpening method using a cylindrical surface consists in the successive forming of the cylindrical surfaces of the flank faces *a, b, c,* using a plane surface d of a grinding wheel, which execute a rotation *A* around its own axis, Figure 4.

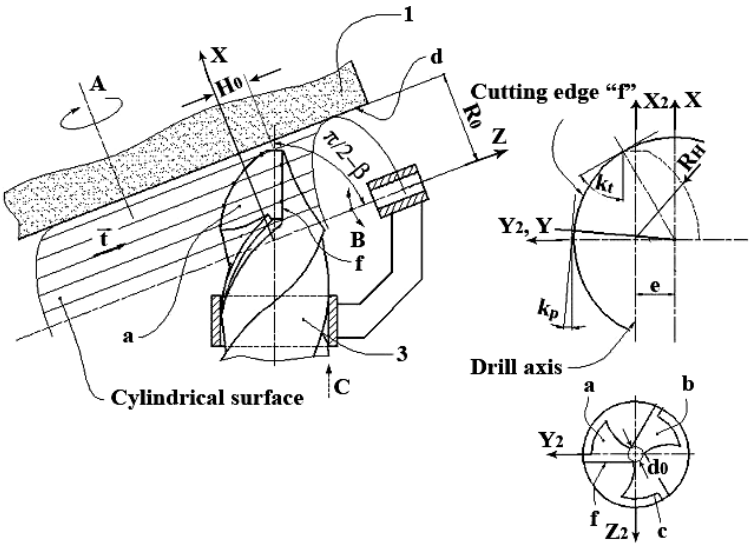

Fig. 4. *The generation kinematics for cylindrical sharpening*

The sharpening of the flank surface of a cutting edge is made by composing the swing motion *B* of the drill, whose axis may be aclived with angle $\left(\frac{\pi}{2}-\beta\right)$ and excentrical with value *e* regarding an axis *z*, parallel with the plane face of the grinding wheel, with an axial feed and intermittent motion *C*, which ensure the relieving of the flank surface, at a single positioning of the sharpened drill.

The cutting edge form results as ellipse $\beta \neq 0$ and is circle if $\beta = 0$.

3. The analytical model of the back angle

3.1. The hyperboloidal model

It is accepted that the hyperboloidal rotation surface is generated by a straight line that belongs to the reference system $X_1Y_1Z_1$ which has the following parametric equations, Figure 2:

$$\Delta_{X_1Y_1Z_1} : \begin{vmatrix} X_1 = u \cdot \sin\lambda; \\ Y_1 = 0; \\ Z_1 = u \cdot \cos\lambda, \end{vmatrix} \quad (1)$$

with *u* variable parameter. In the rotating motion around the *Z* axis (*Z* – hyperboloid's axis), of variable parameter φ, with R_0 and λ - design values:

$$X = \omega_3^T(\varphi) \cdot \left[X_1 - \begin{pmatrix} 0 \\ -R_0 \\ 0 \end{pmatrix} \right], \quad (2)$$

After substitution,

$$\begin{pmatrix} X \\ Y \\ Z \end{pmatrix} = \begin{pmatrix} \cos\varphi & -\sin\varphi & 0 \\ \sin\varphi & \cos\varphi & 0 \\ 0 & 0 & 1 \end{pmatrix} \cdot \begin{pmatrix} u \cdot \sin\lambda \\ R_0 \\ u \cdot \cos\lambda \end{pmatrix}, \quad (3)$$

the family of straight lines is generated – the hyperboloidal surface:

$$\begin{aligned} X &= u \cdot \sin\lambda \cdot \cos\varphi - R_0 \cdot \sin\varphi; \\ Y &= u \cdot \sin\lambda \cdot \sin\varphi + R_0 \cdot \cos\varphi; \\ Z &= u \cdot \cos\lambda. \end{aligned} \quad (4)$$

The (4) equations represent the analytical model of the setting surface of the drill's main edge with curved edges.

The back angle, α_{r_x}, is defined in a plane parallel to the drill's axis, in the measuring plane - normal plane on the base constructive plane, in the point considered on the cutting edge, Figure 5.

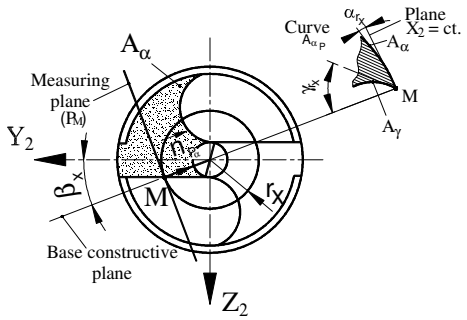

Fig. 5. *The measuring plane*

The base plane, the plane that contains the considered point, is in a point of the cutting edge and it is normal on the direction of the cutting motion, (the speed's direction in point M, in the rotation movement of the drill).

The plane's equation P_{M-} parallel plane with the drill's axis (X_2 axis) is (5):

$$P_M : \left(Y_2 - \sqrt{r_x^2 + \frac{d_0^2}{4}} \right) \cdot cos\,\beta_x + \left(Z_2 - \frac{d_0}{2} \right) \cdot \cdot sin\,\beta_x = 0, \tag{5}$$

with

$$\beta_x = arcsin\left(\frac{d_0}{2 \cdot r_x} \right). \tag{6}$$

The hyperboloidal surface is related to the $X_2Y_2Z_2$ system through the transformation, see Figure 2:

$$\begin{pmatrix} X_2 \\ Y_2 \\ Z_2 \end{pmatrix} = \begin{pmatrix} X \\ Y \\ Z \end{pmatrix} - \begin{pmatrix} 0 \\ e \\ -d_0/2 \end{pmatrix}. \tag{7}$$

Thus, the equations of the hyperboloidal surface – forming the back face of the main curvilinear edge of the drill, in the $X_2Y_2Z_2$ system, have the configuration:

$$A_\alpha : \begin{vmatrix} X_2 = u \cdot sin\,\lambda \cdot cos\,\varphi - R_0 \cdot sin\,\varphi; \\ Y_2 = u \cdot sin\,\lambda \cdot sin\,\varphi + R_0 \cdot cos\,\varphi - e\,; \\ Z_2 = u \cdot cos\,\lambda + d_0/2, \end{vmatrix} \tag{8}$$

with u and φ - independent variable parameters.

The sizes R_0, e, λ, d_0 are definable as constructive sizes (technological constants).

The intersection of surfaces – the measuring plane (5) and the hyperboloid (8) – both defined in the same system of reference, leads to the condition (9):

$$\left(u \cdot sin\,\lambda \cdot sin\,\varphi + R_0 \cdot cos\,\varphi - e - \sqrt{r_x^2 - \frac{d_0^2}{4}} \right) \cdot \cdot cos\,\beta_x + u \cdot cos\,\lambda \cdot sin\,\beta_x = 0. \tag{9}$$

$$H_0 = \frac{\sqrt{R_H^2 - e^2}}{tg\,\lambda} - \frac{d_0}{2} \tag{10}$$

Independent variable parameter u is:

$$u = \frac{\left(-R_0 \cdot cos\,\varphi + e + \sqrt{r_x^2 - \frac{d_0^2}{4}} \right) \cdot cos\,\beta_x}{sin\,\lambda \cdot sin\,\varphi \cdot cos\,\beta_x + cos\,\lambda \cdot sin\,\beta_x}. \tag{11}$$

The equations of the hyperboloidal surface in the $X_2Y_2Z_2$ system become (12):

$$X_2 = \frac{\left(-R_0 \cdot cos\,\varphi + e + \sqrt{r_x^2 - \frac{d_0^2}{4}} \right) \cdot cos\,\beta_x}{sin\,\lambda \cdot sin\,\varphi \cdot cos\,\beta_x + cos\,\lambda \cdot sin\,\beta_x} \cdot \cdot sin\,\lambda \cdot cos\,\varphi - R_0 \cdot sin\,\varphi;$$

$$Y_2 = \frac{\left(-R_0 \cdot cos\,\varphi + e + \sqrt{r_x^2 - \frac{d_0^2}{4}} \right) \cdot cos\,\beta_x}{sin\,\lambda \cdot sin\,\varphi \cdot cos\,\beta_x + cos\,\lambda \cdot sin\,\beta_x} \cdot \cdot sin\,\lambda \cdot sin\,\varphi + R_0 \cdot cos\,\varphi - e; \tag{12}$$

$$Z_2 = \frac{\left(-R_0 \cdot cos\,\varphi + e + \sqrt{r_x^2 - \frac{d_0^2}{4}} \right) \cdot cos\,\beta_x}{sin\,\lambda \cdot sin\,\varphi \cdot cos\,\beta_x + cos\,\lambda \cdot sin\,\beta_x} \cdot \cdot cos\,\lambda + d_0/2,$$

3.2. The conical model

For the conical model, see Figure 3, from the equations (8), for $R_0 = 0$, and

$$H_0 = \frac{R_H}{tg\,\lambda} - \frac{d_0}{2} \tag{13}$$

we obtain the conical surface:

$$A_\alpha : \begin{vmatrix} X_2 = u \cdot sin\,\lambda \cdot cos\,\varphi; \\ Y_2 = u \cdot sin\,\lambda \cdot sin\,\varphi - e\,; \\ Z_2 = u \cdot cos\,\lambda + d_0/2. \end{vmatrix} \tag{14}$$

The similar condition (9) for conical model is:

$$\left(u \cdot sin\,\lambda \cdot sin\,\varphi - e - \sqrt{r_x^2 - \frac{d_0^2}{4}} \right) \cdot \cdot cos\,\beta_x + u \cdot cos\,\lambda \cdot sin\,\beta_x = 0. \tag{15}$$

Independent variable parameter u is:

$$u = \frac{\left(e + \sqrt{r_x^2 - \frac{d_0^2}{4}}\right) \cdot \cos\beta_x}{\sin\lambda \cdot \sin\varphi \cdot \cos\beta_x + \cos\lambda \cdot \sin\beta_x} \tag{16}$$

and the conical surface becomes:

$$X_2 = \frac{\left(e + \sqrt{r_x^2 - \frac{d_0^2}{4}}\right) \cdot \cos\beta_x}{\sin\lambda \cdot \sin\varphi \cdot \cos\beta_x + \cos\lambda \cdot \sin\beta_x} \cdot \cdot \sin\lambda \cdot \cos\varphi;$$

$$Y_2 = \frac{\left(e + \sqrt{r_x^2 - \frac{d_0^2}{4}}\right) \cdot \cos\beta_x}{\sin\lambda \cdot \sin\varphi \cdot \cos\beta_x + \cos\lambda \cdot \sin\beta_x} \cdot \cdot \sin\lambda \cdot \sin\varphi - e; \tag{17}$$

$$Z_2 = \frac{\left(e + \sqrt{r_x^2 - \frac{d_0^2}{4}}\right) \cdot \cos\beta_x}{\sin\lambda \cdot \sin\varphi \cdot \cos\beta_x + \cos\lambda \cdot \sin\beta_x} \cdot \cdot \cos\lambda + d_0 / 2.$$

3.3. The cylindrical model

For the cylindrical model, see Figure 4, from the equations (8), for

$$R_0 = R_H\ ,\ \lambda = 0\ , \tag{18}$$

$$R_H = \frac{\sqrt{\frac{D^2}{4} - \frac{d_0^2}{4}}}{\cos\chi_p - \cos\chi_t}\ , \tag{19}$$

$$e = R_H \cdot \cos\chi_t\ , \tag{20}$$

$$H_0 = -\frac{d_0}{2}\ , \tag{21}$$

we obtain the cylindrical surface:

$$A_\alpha : \begin{vmatrix} X_2 = -R_H \cdot \sin\varphi; \\ Y_2 = R_H \cdot \cos\varphi - e; \\ Z_2 = u + d_0 / 2. \end{vmatrix} \tag{22}$$

The similar condition (9) for cylindrical model is:

$$\left(R_0 \cdot \cos\varphi - e - \sqrt{r_x^2 - \frac{d_0^2}{4}}\right) \cdot \cdot \cos\beta_x + u \cdot \sin\beta_x = 0. \tag{23}$$

Independent variable parameter u is:

$$u = \frac{\left(-R_0 \cdot \cos\varphi + e + \sqrt{r_x^2 - \frac{d_0^2}{4}}\right) \cdot \cos\beta_x}{\sin\beta_x} \tag{24}$$

and the cylindrical surface becomes:

$$X_2 = -\frac{\sqrt{\frac{D^2}{4} - \frac{d_0^2}{4}}}{\cos\chi_p - \cos\chi_t} \cdot \sin\varphi;$$

$$Y_2 = \frac{\sqrt{\frac{D^2}{4} - \frac{d_0^2}{4}}}{\cos\chi_p - \cos\chi_t} \cdot \sin\varphi \cdot \cos\varphi - e; \tag{25}$$

$$Z_2 = \frac{\left(-R_0 \cdot \cos\varphi + e + \sqrt{r_x^2 - \frac{d_0^2}{4}}\right) \cdot \cos\beta_x}{\sin\beta_x} + + d_0 / 2.$$

The ensemble of equations created from the setting surface (8), (14), (22) and respectively conditions (9), (15), (23) and the equations of the intersection curves of the setting surfaces with the measuring plane P_M will define the α_{r_x} angle, see Figure 5.

4. Numerical applications

There are presented applications of the algorithm for the determination of the flank angle for the three sharpening methods, in the conditions of respecting the major cutting edge geometry.

$$\chi_p = 5^\circ;\ \chi_t = 60^\circ;\ D_b = 20\ mm;\ d_0 = 2{,}4\ mm.$$

In Figures 6, 7 and 8, are presented the values for the flank angle, along the major cutting edge for all of the three presented methods.

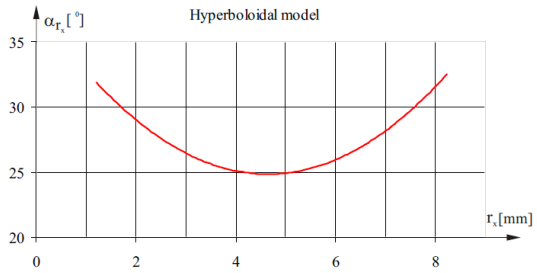

Fig. 6. *Variation law for the back angle size - hyperboloidal model*

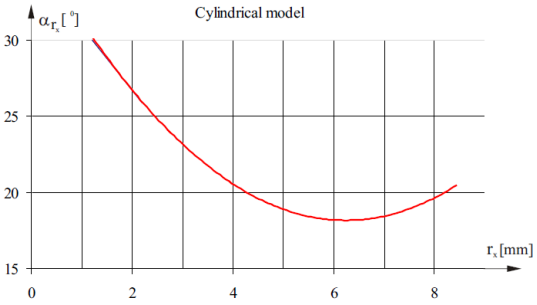

Fig. 7. *Variation law for the back angle size - cylindrical model*

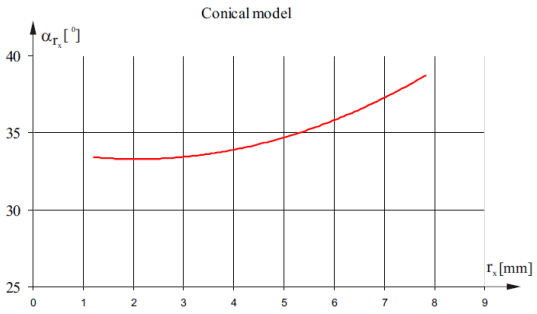

Fig. 8. *Variation law for the back angle size - conical model*

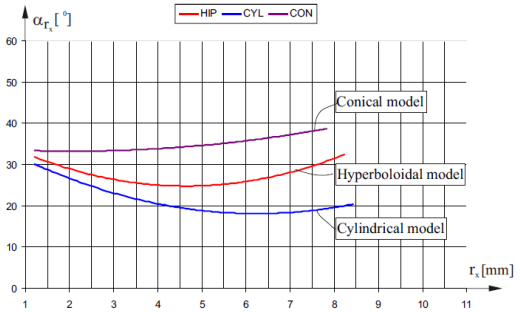

Fig. 9. *Variation law for the back angle size – hyperboloidal, cylindrical and conical model*

5. Conclusions

The presented methods allow determining the value of the flank angle, along the major cutting edge, according to the accepted definition. For all of the analysed sharpening method, the flank angle has values according to the tool's type requirements. The hyperboloidal method ensures the largest value of the flank angle at drill periphery. The constructive parameters modification, the increasing of the working cutting edge angle, at drill periphery, κ_p, and at drill top, κ_t, as well as the core diameter of drill, $d = 0.12 \cdot D$, have influence on the law of flank angle variation.

REFERENCES

[1]. Baroiu, N., Berbinschi, S., Teodor, V., Fetecău, C., Oancea, N., *Hyperboloidal sharpening method for multi flute curved edges drills*, The Annals of "Dunărea de Jos" University of Galați, Fascicle V, Technologies in Machine Building, ISSN 1221-4566, 2010, pp. 117-124.

[2]. Fetecău, C, Stan, F, Oancea, N., *Toroidal Grinding Method for Curved Cutting Edge Twist Drills*, Journal of Material Processing Technology, Nr. 209, 2009, pp. 3460-3468.

[3]. Fetecău, C., Teodor,V., Dumitraşcu, N., Oancea, N., *Method for Conical Sharpening of Multi-Flute Helical Drill with curved Cutting Edge*, Proceedings of the 14 th International Conference ModTech, ISSN 2066-3919, 2010, pp. 275-278.

[4]. Teodor,V. Fetecău, C., Oancea, N., Dumitraşcu, N., Marinescu, V., Patent RO125839-A2, 2010.

Modele analitice comparative ale procedeelor de ascuțire a burghielor multi-tăiş cu tăişuri curbe

—Rezumat—

Lucrarea prezintă, comparativ, trei procedee de ascuțire pentru burghiele elicoidale cu mai multe tăişuri curbe, şi anume: ascuțirea hiperboloidală, cilindrică şi conică. Modelele analitice ale muchiei de aşchiere şi ale formelor suprafețelor de aşezare sunt analizate din prisma îndeplinirii cerințelor minime ale unui procedeu de ascuțire a burghielor: asigurarea mărimii unghiului de aşezare în lungul muchiei de aşchiere. Cinematica celor trei procedee de ascuțire este simplă şi comparabilă cu cinematica procedeelor de ascuțire cunoscute pentru burghiele standard, iar prin exemplele numerice analizate, se observă modul în care variază unghiul de aşezare în lungul tăişului principal, în sensul creşterii mărimii unghiului de aşezare de la periferie către vârf.